Shear Viscosity and Shear Thinning in Two-Dimensional Yukawa Liquids

Z. Donkó,[1] J. Goree,[2] P. Hartmann,[1] and K. Kutasi[1]

[1]*Research Institute for Solid State Physics and Optics of the Hungarian Academy of Sciences, H-1525 Budapest, P.O. Box 49, Hungary*
[2]*Department of Physics and Astronomy, The University of Iowa, Iowa City, Iowa 52242, USA*

A two-dimensional Yukawa liquid is studied using two different nonequilibrium molecular dynamics simulation methods. Shear viscosity values in the limit of small shear rates are reported for a wide range of Coulomb coupling parameter and screening lengths. At high shear rates it is demonstrated that this liquid exhibits shear thinning; i.e., the viscosity η diminishes with increasing shear rate. It is expected that two-dimensional dusty plasmas will exhibit this effect.

Many-particle systems characterized by the Yukawa potential include a variety of physical systems, e.g., dusty plasmas, charged colloids, astrophysical objects, and high energy density matter. The Yukawa potential $\phi(r) \propto Q \exp(-r/\lambda_D)/r$ models a Coulomb repulsion that is exponentially suppressed with a screening length λ_D. Yukawa systems behave like a liquid when the temperature exceeds a melting point which depends on Q, λ_D, and particle spacing, e.g., [1,2].

Transport parameters of Yukawa systems—the diffusion coefficient [3], the shear viscosity [4–6], and the thermal conductivity [6,7]—have mainly been calculated for 3D systems, but there is now an increasing interest in 2D settings. For example, in dusty plasma experiments, charged microspheres suspended as a monolayer in a gas discharge make a 2D Yukawa system. By creating a shear flow in such a particle suspension, the viscosity was measured in recent experiments using 2D suspensions [8] and quasi-2D suspensions consisting of a few monolayers of charged microspheres [9]. The transport properties of such ultrathin liquids are also of interest as macroscopic analogs of molecular flow in nanoscience applications [10].

Transport coefficients are meaningful if they are part of a valid "constitutive relation" between the gradients of local variables and fluxes. For shear viscosity η, the constitutive relation $j_y = -\eta[dv_x(y)/dy]$ relates a momentum flux j_y to the velocity gradient $dv_x(y)/dy$, which is also termed the shear rate. In a non-Newtonian fluid, η may vary with the velocity gradient, whereas in Newtonian fluids it does not. In particular, if η diminishes as shear is increased, the fluid is said to exhibit "shear thinning." This occurs in simple liquids [11], as well as in complex mixtures such as foams, micelles, slurries, pastes, gels, polymer solutions, and granular flows [12]. Recently, experimenters have claimed to observe shear thinning in dusty plasma liquids [9]. These reports motivate our simulations to search for the presence of shear thinning in 2D Yukawa liquids.

Subsequent to the experimental measurement of viscosity in a 2D dusty plasma [8], a 2D molecular dynamics simulation was used to obtain the shear viscosity from the Green-Kubo relations [13]. In this Letter we will go beyond the results of Ref. [13], which were performed for equilibrium conditions, by using nonequilibrium simulations to search for non-Newtonian behavior under conditions of a high shear rate. We will also compute the viscosity over a wider range of Γ and κ.

Our simulations use a rectangular cell with edge lengths L_x and L_y and periodic boundary conditions. The number of particles is between $N = 990$ and 7040. The system is characterized by dimensionless parameters $\Gamma = Q^2/4\pi\varepsilon_0 a k_B T$ and $\kappa = a/\lambda_D$, where $a = (1/n\pi)^{1/2}$ is the Wigner-Seitz radius, with n being the areal density. Additional parameters include the thermal velocity $v_0 = (2k_B T/m)^{1/2}$ and the 2D analog of the plasma frequency $\omega_p = (Q^2/2\pi\varepsilon_0 m a^3)^{1/2}$, the shear rate $\gamma = dv_x/dy$, and its normalized value $\bar{\gamma} = (dv_x/dy)(a/v_0)$. Two types of molecular dynamics techniques are applied for the studies of the shear viscosity.

Method 1 reverses the cause-and-effect picture customarily used in nonequilibrium molecular dynamics: the effect—the momentum flux—is imposed, and the cause—the velocity gradient (shear rate)—is measured in the simulation [14]. Momentum in the liquid is introduced in a pair of narrow slabs A and B, which are centered at $y = L_y/4$ and $3L_y/4$, respectively. At regular time intervals τ we identify the particles in slabs A and B having the highest $|v_x|$ in the positive and negative directions, respectively. We then instantaneously exchange the v_x velocity component of these two particles without moving the particles. This artificial transfer of momentum between slabs A and B (which is accomplished without changing the system energy) produces a velocity profile $v_x(y)$, the slope of which can be controlled by the frequency of the momentum exchange steps. The equations of motion

$$\frac{d\mathbf{r}_i}{dt} = \frac{\mathbf{p}_i}{m}, \qquad \frac{d\mathbf{p}_i}{dt} = \mathbf{F}_i, \qquad (1)$$

where $\mathbf{r} = (x, y)$, $\mathbf{p} = (p_x, p_y)$ are the positions and the momenta of particles, m is their mass, and $\mathbf{F}_i$ is the force

acting on particle i, are integrated by the velocity Verlet algorithm.

Method 2 simulates a planar Couette flow, which is established by the Lees-Edwards periodic boundary conditions resulting in a homogeneous streaming flow field in the simulation box: $\langle v_x \rangle = \gamma(y - L_y/2)$, where $\langle \rangle$ denotes a time average. The system is described by the Gaussian thermostated SLLOD equations of motion [15]:

$$\frac{d\mathbf{r}_i}{dt} = \frac{\tilde{\mathbf{p}}_i}{m} + \gamma y_i \hat{\mathbf{x}}, \qquad \frac{d\tilde{\mathbf{p}}_i}{dt} = \mathbf{F}_i - \gamma \tilde{p}_{yi} \hat{\mathbf{x}} - \alpha \tilde{\mathbf{p}}_i, \quad (2)$$

where $\tilde{\mathbf{p}} = (\tilde{p}_x, \tilde{p}_y)$ is the *peculiar* momentum of particles, $\hat{\mathbf{x}}$ is the unit vector in the x direction, and α is the Gaussian thermostating multiplier. The above set of equations is solved using an operator splitting technique [16].

In contrast to method 1, method 2 results in a homogeneous shear field and a constant temperature within the whole simulation box. Thus, arbitrarily high shear rates may be established without the need of considering any effects of temperature gradients on the viscosity.

In both methods the pairwise Yukawa interparticle forces are summed over a κ-dependent cutoff radius, using the chaining mesh technique. (The force due to particles at the cutoff radius is $\approx 10^{-5}$ smaller compared to that due to the nearest neighbors.) Both methods neglect any neutral gas drag, which has been observed to alter the velocity profiles in experiments [8], i.e., they model an atomic system where momentum transfer is dominated by Coulomb collisions [1].

Method 1 has the advantage that resembles more closely the experimental conditions, although the procedure for applying shear in the simulation involves no introduction or removal of energy from the system. In the experiment [8] shear is applied via an external introduction of both momentum and energy in a boundary slab while energy is simultaneously removed elsewhere by frictional dissipation. Method 2 represents a well-established technique for measurement of viscosity at arbitrary steady, as well as temporally varying shear rates. Although it has little connection to the conditions found in the experiment, it has been demonstrated to be an efficient technique to investigate shear thinning [11,15]. Thus we apply this method for the studies of this latter effect.

Near-equilibrium (small γ) shear viscosity values have been obtained using both techniques. In method 1 this is done at the lowest practical shear rate, where dv_x/dy is uniform between slabs A and B. We calculate η_{eq} from

$$|j_y| = \eta_{\text{eq}} dv_x(y)/dy = \Delta p/2 t_{\text{sim}} L_y, \quad (3)$$

where Δp is the total x-directional momentum exchanged between slabs A and B during the simulation time t_{sim} [14]. In method 2 the off-diagonal element of the pressure tensor is measured during the course of the simulation:

$$P^{xy}(t) = \sum_{i=1}^{N}\left[m v_{ix} v_{iy} + \sum_{j>i}^{N} \frac{x_{ij} y_{ij}}{r_{ij}} \frac{d}{dr_{ij}} \phi(r_{ij}) \right], \quad (4)$$

where $\mathbf{r}_{ij} = \mathbf{r}_i - \mathbf{r}_j = (x_{ij}, y_{ij})$, and the shear viscosity is obtained as

$$\eta = \lim_{t \to \infty} \langle P^{xy}(t) \rangle / \gamma. \quad (5)$$

In method 1, the spatial profiles for temperature and velocity, Fig. 1, develop self-consistently in response to the perturbation applied by introducing momentum in slabs A and B. We use method 1 only for small perturbations, so that the velocity profile has a linear gradient and the temperature is isotropic, with $T_x = T_y$, where $T_{x,y} = (m/N_j k_B) \sum_{i=1}^{N_j} \langle [v_{ix,y}(t) - \overline{v_{jx,y}}]^2 \rangle$. The index i runs over the N_j particles in slab j. We verified that $\overline{v_{jy}}$ is negligibly small.

Obtaining reliable results for η at small γ requires a simulation duration of typically $\omega_p t \sim 10^4$–10^5 for both methods. The required time step is smallest and the simulations are most costly at low Γ. In method 1, system size effects are expected to appear when (i) particles traverse the simulation box without significant interaction with the others, or (ii) the compressional sound wave transits the box in a shorter time than the decay time t_c of the velocity autocorrelation function. For (i), for our most demanding condition (small size $N = 990$ and high temperature $\Gamma = 1$) a particle moving at the thermal velocity would transit the cell in a time $\omega_p t \approx 57$ if it were undeflected by collisions. We find that the decay time is short enough, $\omega_p t_c \sim 5$–10, even for the smallest Γ values of interest. Thus we expect no "ballistic" trajectories across the entire simulation box. For (ii), the sound speed [17] at $\kappa = 1$ is $v = d\omega/dk \sim a\omega_p$, and the wave's transit time Δt across a
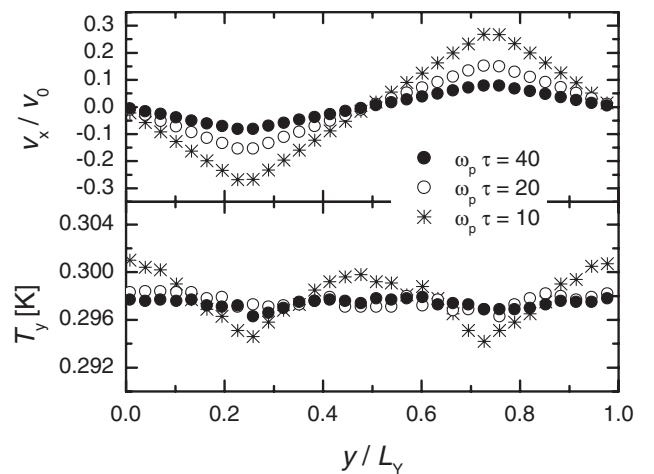

FIG. 1. (a) Velocity profiles $v_x(y)$ obtained from method 1 for different frequencies ($1/\tau$) of momentum exchange steps, and (b) $T_y(y)$ temperature profiles for the same conditions. $\Gamma = 100$, $\kappa = 1$.
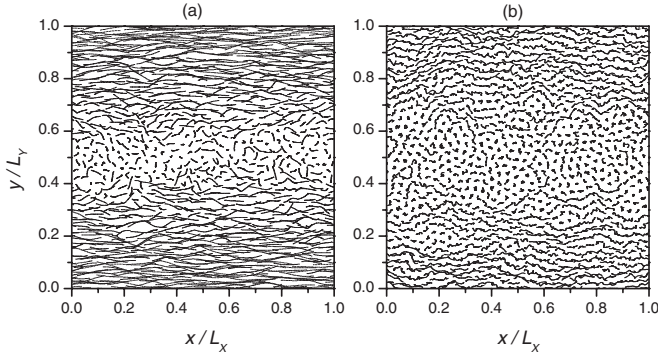
FIG. 2.   (a) Trajectories of particles in the simulation based on method 2. (a) $\Gamma = 10$, $\kappa = 1$ at a shear rate $\bar{\gamma} = 0.2$; time of recording: $\omega_p \Delta T = 5.0$.   (b) $\Gamma = 100$, $\kappa = 1$, $\bar{\gamma} = 0.05$, $\omega_p \Delta T = 23.6$. The shear field is $v_x = \gamma(y - L_y/2)$, i.e., there is no flow at $y = L_y/2$. $N = 1020$.

box with length L_y is $\omega_p \Delta t \sim L_y/a = 57$ for our most demanding case, $N = 990$ particles. Thus, we find both criteria fulfilled for a "sufficiently large" system. Method 2 is known to produce accurate results even for the small number of particles simulated [15]. We verified that the results obtained from both methods did not depend significantly on N.

Figures 2(a) and 2(b) illustrate particle trajectories in simulations based on method 2, for conditions $\Gamma = 10$, $\kappa = 1$ at a shear rate $\bar{\gamma} = 0.2$, and for $\Gamma = 100$, $\kappa = 1$, $\bar{\gamma} = 0.05$, respectively.

Our results for η_{eq} as a function of Γ, for different values of κ are plotted in Fig. 3(a). We find a good agreement with the earlier equilibrium molecular-dynamic (MD) simulation of Ref. [13]. In contrast with most simple liquids, which have a viscosity that varies monotonically with temperature, a prominent feature of the viscosity of the present system is a minimum (e.g., at $\Gamma \cong 20$ for $\kappa = 1$), which has been noted previously in both one-component plasma (OCP) and Yukawa liquids. The shape of the $\eta_{eq}(\Gamma)$ curve can be explained by the prevailing kinetic and potential contributions to the viscosity at low and high values of Γ, respectively. The near-equilibrium shear viscosity values obtained with method 2 for $\kappa = 1$ are also displayed Fig. 3(a). We find an excellent agreement between the results of methods 1 and 2.

Similar to what was observed in [5] for 3D Yukawa liquids, we find that the near-equilibrium viscosity η_{eq} obeys a scaling law as demonstrated in Fig. 3(b), where viscosity has been normalized by $\eta_E = mn\omega_E a^2$. The Einstein frequency ω_E depends on κ, and we computed it from Eq. (7) of Ref. [17] using pair-correlation functions measured from our simulations. The horizontal axis is a normalized temperature $T' = T_y/T_m = \Gamma_m/\Gamma$, where T_m and Γ_m are melting-point values reported in Ref. [2]. Using these normalizations, the data fall on the same curve, demonstrating the existence of a scaling law for the $0.5 \leq$
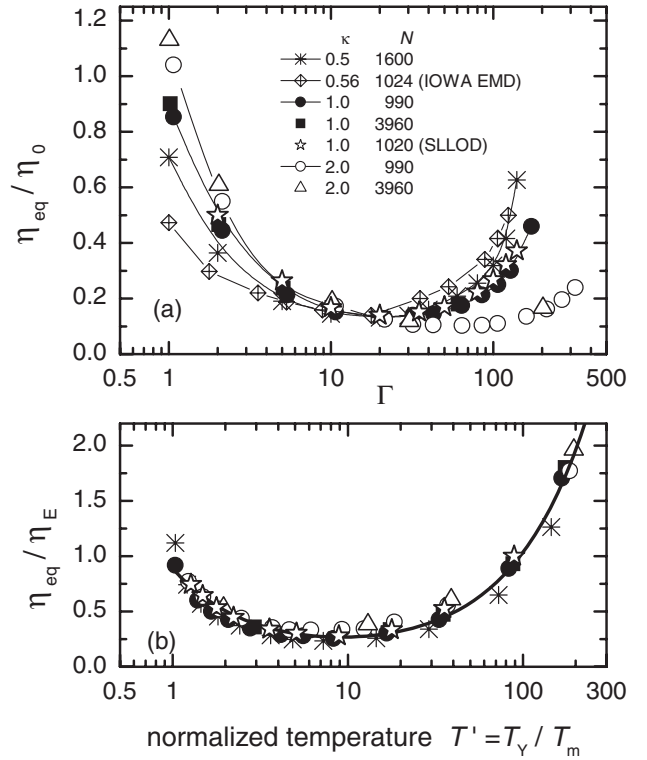

FIG. 3.   (a) Shear viscosity at near-equilibrium conditions, η_{eq}, obtained from method 1, at the simulation's lowest practical shear rate, and normalized by $\eta_0 = mn\omega_p a^2$. For comparison, data are shown from the Iowa equilibrium MD simulation [13] and from simulations based on method 2 (SLLOD), in the limit of small shear rates, at $\kappa = 1$. N is the number of simulation particles. (b) A scaling law is demonstrated by normalizing the data in (a) using $\eta_E = mn\omega_E a^2$ and $T' = T_y/T_m$, where T_m is the melting temperature. The thick line is an empirical fit of form $\eta_{eq}/\eta_E = aT' + b/T' + c$.

$\kappa \leq 2.0$ range of the screening parameter. We note that for this purpose we found ω_E was more significant than ω_p. The near-equilibrium viscosity is fit by an empirical form (like in [5] for three dimensions) $\eta_{eq}/\eta_E = aT' + b/T' + c$ with coefficients: $a = 0.0093$, $b = 0.78$, and $c = 0.098$.

A shear-thinning effect is revealed in Fig. 4(a), which shows that η diminishes significantly as the shear rate $\bar{\gamma}$ is increased. In other two-dimensional systems the reduction in η, as compared to the value at small shear, was observed to vary as the square root of $\bar{\gamma}$ [11]. We find that this scaling also occurs for the Yukawa system, as indicated by data that fall on nearly straight lines in Fig. 4(a) for $\bar{\gamma} > 0.2$. At smaller shear rates, $\bar{\gamma} < 0.2$, however, the shear-thinning effect is less profound and the liquid is more nearly Newtonian, especially for large Γ. Results are shown for $\bar{\gamma} \gtrsim 0.01$, which we found to be reliable, whereas at lower $\bar{\gamma}$, method 2 yielded noisy data even for very long simulations.

Because viscosity arises from both kinetic and potential contributions, Eq. (4), we evaluate which of these contri-
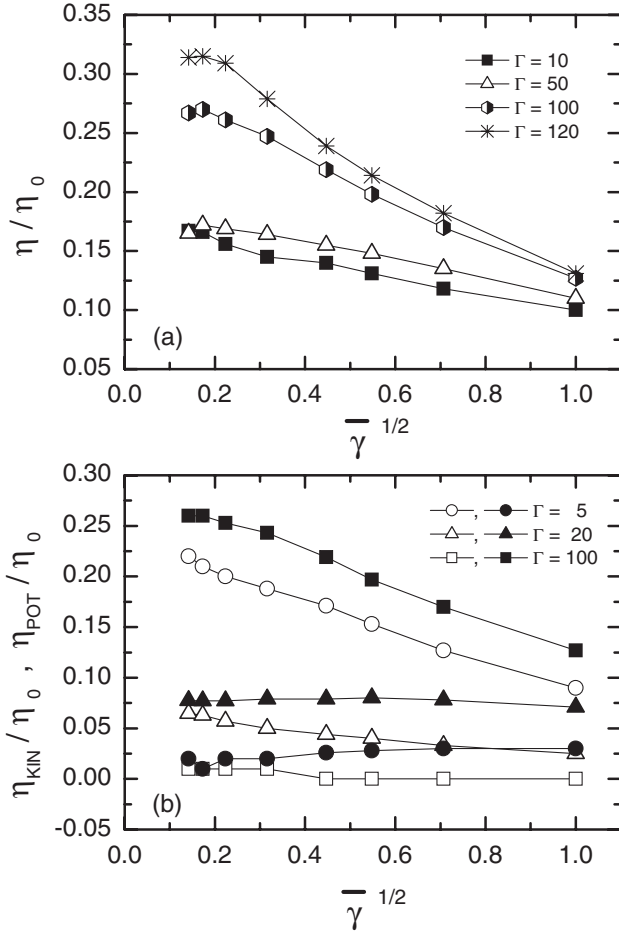
FIG. 4. (a) Shear viscosity as a function of normalized shear rate $\bar{\gamma}$ for selected values of the coupling parameter Γ. (b) Potential (solid symbols) and kinetic (open symbols) contributions to the shear viscosity. $\kappa = 1$.

butions is most responsible for the observed shear-thinning effect in Fig. 4(b). Recall that for equilibrium conditions, the kinetic term dominates for $\Gamma \ll 20$ and the potential term dominates for $\Gamma \gg 20$. Here, we find that for non-equilibrium conditions, as the shear rate increases the reduction in viscosity is mostly due to a reduction of the kinetic contribution at low Γ and a reduction of the potential contribution at high Γ. In other words, at extreme values of Γ, it is the same term dominating the equilibrium viscosity that also dominates the shear-thinning effect. At an intermediate value of $\Gamma = 20$, however, where the equilibrium viscosity has a minimum and the two equilibrium contributions are comparable (for $\kappa = 1$), we find that it is mostly a reduction of the kinetic term that accounts for the observed shear-thinning effect.

In summary, we have calculated the shear viscosity coefficient of 2D Yukawa liquids in a wide domain of parameters Γ and κ using two different molecular dynamics approaches. The small shear rate calculations confirmed that the two techniques used are consistent and

yielded η values in fair agreement with equilibrium MD calculations [13]. The small shear rate data were found to obey a universal scaling: η normalized by the Einstein frequency was found to depend only on the reduced temperature (ratio of the temperature to melting temperature). The high shear rate simulations based on method 2 unambiguously demonstrated a non-Newtonian behavior of the Yukawa liquid: η was significantly reduced for these conditions in a manifestation of shear thinning, except at the lowest shear rates where the liquid is more nearly Newtonian. Regimes of the plasma coupling parameter were identified to distinguish whether the kinetic or potential contribution to the shear viscosity is primarily responsible for the shear-thinning effect.

[1] S. A. Khrapak, A. V. Ivlev, and G. E. Morfill, Phys. Rev. E **70**, 056405 (2004).
[2] P. Hartmann, G. J. Kalman, Z. Donkó, and K. Kutasi, Phys. Rev. E **72**, 026409 (2005).
[3] H. Ohta and S. Hamaguchi, Phys. Plasmas **7**, 4506 (2000).
[4] K. Y. Sanbonmatsu and M. S. Murillo, Phys. Rev. Lett. **86**, 1215 (2001).
[5] T. Saigo and S. Hamaguchi, Phys. Plasmas **9**, 1210 (2002).
[6] G. Salin and J.-M. Caillol, Phys. Rev. Lett. **88**, 065002 (2002); G. Faussurier and M. S. Murillo, Phys. Rev. E **67**, 046404 (2003).
[7] Z. Donkó and P. Hartmann, Phys. Rev. E **69**, 016405 (2004).
[8] V. Nosenko and J. Goree, Phys. Rev. Lett. **93**, 155004 (2004).
[9] C.-L. Chan, W.-Y. Woon, and L. I, Phys. Rev. Lett. **93**, 220602 (2004).
[10] S. Granick, Phys. Today **52**, No. 7, 26 (1999); Subrata Roy *et al.*, J. Appl. Phys. **93**, 4870 (2003).
[11] D. J. Evans, Phys. Rev. A **23**, 1988 (1981).
[12] A. Kabla and G. Debregeas, Phys. Rev. Lett. **90**, 258303 (2003); J. B. Salmon, A. Colin, S. Manneville, and F. Molino, Phys. Rev. Lett. **90**, 228303 (2003); F. Varnik, L. Bocquet, J.-L. Barrat, and L. Berthier, Phys. Rev. Lett. **90**, 095702 (2003); Y. Jiang *et al.*, Phys. Rev. E **59**, 5819 (1999).
[13] Bin Liu and J. Goree, Phys. Rev. Lett. **94**, 185002 (2005).
[14] F. Müller-Plathe, Phys. Rev. E **59**, 4894 (1999).
[15] D. J. Evans and G. P. Morriss, *Statistical Mechanics of Nonequilibrium Liquids* (Academic, New York, 1990).
[16] G. Pan, J. F. Ely, C. McCabe, and D. J. Isbister, J. Chem. Phys. **122**, 094114 (2005).
[17] G. J. Kalman, P. Hartmann, Z. Donkó, and M. Rosenberg, Phys. Rev. Lett. **92**, 065001 (2004).